International Journal of Cardiology 278 (2019) 76–83

Contents lists available at ScienceDirect

International Journal of Cardiology

journal homepage: www.elsevier.com/locate/ijcard

Prognostic value of echocardiographic parameters in pediatric patients with Ebstein's anomaly☆

Costantina Prota [a,b], Giovanni Di Salvo [a,*], Jolanda Sabatino [a], Manjit Josen [a], Josefa Paredes [a], Domenico Sirico [a], Marisol Uy Pernia [a], Andreas Hoschtitzky [a], Guido Michielon [a], Rodolfo Citro [b], Alain Fraisse [a], Olivier Ghez [a]

[a] Paediatric Cardiology, Royal Brompton Hospital, London, United Kingdom
[b] Heart Department, University Hospital San Giovanni di Dio e Ruggi d'Aragona, Salerno, Italy

ARTICLE INFO

Article history:
Received 11 June 2018
Received in revised form 12 September 2018
Accepted 12 October 2018
Available online 14 October 2018

Keywords:
Ebstein's anomaly
Pediatric population
Echocardiography
Speckle tracking echocardiography
Outcome

ABSTRACT

Background: Accurate risk stratification of patients with Ebstein's anomaly (EA) is crucial. Aim of the study was to assess the prognostic value of echocardiography, including 2D speckle tracking (STE) derived myocardial deformation indices, for predicting outcome in pediatric and young adult unrepaired EA patients.
Methods: Fifty consecutive EA patients (1 day–18 years, 52% males) underwent echocardiography and were followed for a mean follow-up of 60 ± 41 months for clinical outcome (ventricular tachyarrhythmia, heart failure, need for surgery and/or death). Clinical and instrumental features of EA patients with stable disease were compared with those of EA patients with progressive disease.
Results: Twenty-four (48%) EA patients had progressive disease. A more severe grade of tricuspid valve (TV) displacement [59.7 mm/m^2 (IQR 27.5–83) vs 28.4 mm/m^2 (IQR 17.5–47); $p = 0.002$], a lower functional right ventricle (RV) fractional area change (FAC) (29.2 ± 7.7% vs 36.7 ± 9.6%; $p = 0.004$), a higher Celermajer index [0.8 (IQR 0.7–0.98) vs 0.55 (IQR 0.4–0.7); $p = 0.000$], a lower functional RV-longitudinal strain (−10.2 ± 6.2% vs −16.2 ± 7.3%; $p = 0.003$) and a lower right atrium peak systolic strain (RA-PALS) (25.2 ± 13.5% vs 36.3 ± 12.5%; $p = 0.004$) were detected in progressive disease group compared to stable one, respectively. Functional RV-FAC and RA-PALS were independent predictors of progressive disease at multivariate analysis.
Conclusion: Our study demonstrated for the first time the prognostic role of RV-FAC and RA-PALS in a long-term follow-up of EA young patients. A complete echocardiographic evaluation should be regular part in the evaluation and risk-stratification of EA children.

1. Introduction

Ebstein's anomaly (EA) is a rare congenital heart disorder with an incidence of about 1 per 200,000 live births, representing <1% of all cases of congenital heart disease [1].

It affects primarily the inflow portion of the right ventricle (RV); the typical displacement of the tricuspid valve (TV) is associated with altered RV geometry and often significant valvular regurgitation [2].

This complex congenital anomaly has a very variable anatomical and clinical spectrum, and can present as a severely symptomatic neonate or sometimes as an asymptomatic adult [3]. Mortality is commonly related to sustained tachyarrhythmia and congestive heart failure [4,5].

Accurate risk stratification of these patients is crucial; several previous studies showed conflicting data on the prognostic role of different clinical and imaging features in EA patients [6–10].

Despite echocardiography being the primary diagnostic tool in the assessment and care of patients with EA [11,12], studies about the prognostic value of echocardiography are scarce even more so in the pediatric population [13,14]. Interestingly, a recent paper comparing echocardiographic assessment of the RV with the gold standard cardiac magnetic resonance (CMR) in EA patients showed that only 2D RV global longitudinal strain correlates with CMR-derived RV ejection fraction [15].

Abbreviations: BSA, Body surface area; CMR, Cardiac magnetic resonance; EA, Ebstein's anomaly; EF, Ejection fraction; FAC, Fractional area change; GLS, Global longitudinal strain; LA, Left atrium; LV, Left ventricle, left ventricular; MAPSE, Mitral annular plane systolic excursion; NYHA, New York Heart Association; PALS, Peak atrial longitudinal strain; RA, Right atrium; RV, Right ventricle, right ventricular; STE, Speckle tracking echocardiography; TAPSE, Tricuspid annular plane systolic excursion; TR, Tricuspid regurgitation; TV, Tricuspid valve.

☆ All authors takes responsibility for all aspects of the reliability and freedom from bias of the data presented and their discussed interpretation.

* Corrisponding author at: Consultant Pediatric Cardiology, Lead Pediatric Cardiology Echo Royal Brompton & Harefield Trust, Imperial College of London, United Kingdom.
E-mail address: g.disalvo@rbht.nhs.uk (G. Di Salvo).

https://doi.org/10.1016/j.ijcard.2018.10.046
0167-5273/

Thus, the aim of the present study was to assess for the first time the prognostic value of echocardiography, including 2D speckle tracking (STE) derived myocardial deformation indices, for predicting outcome in a relatively large cohort of pediatric and young adult (≤18 years) unrepaired EA patients.

2. Methods

2.1. Study population

All pediatric and young adults patients (0–18 years old) with unrepaired Ebstein's Anomaly (EA) followed up at the Royal Brompton Hospital (London, UK) who had consecutively undergone transthoracic echocardiography between January 2005 and December 2017, with adequate digitally stored images available, were retrospectively included in the study.

The diagnosis of EA was established by the characteristic tethering of the septal and inferior leaflets with shift of the functional TV orifice away from the anatomic atrioventricular groove [12]. In particular, EA was defined as apical displacement of the septal leaflet of the TV by at least 8 mm/m^2 as compared to the mitral valve attachment, seen in an apical four-chamber view at echocardiography [16].

Patients with other complex associated congenital heart defects such as transposition of great arteries (1 patient) and congenitally corrected transposition of great arteries associated with RV hypoplasia (1) were excluded from this cohort, whereas patients with additional patent foramen ovale/secundum atrium septal defect (33), small ventricular septal defect (4), patent ductus arteriosus (6), additional ≤ mild valve disease (3) were included in the study.

Demographic and clinical data including sex, age, body surface area (BSA), systolic and diastolic blood pressure, New York Heart Association (NYHA) functional class, transcutaneous oxygen saturation, QRS complex duration and pre-excitation on ECG and chest x-ray cardiothoracic ratio were all obtained from medical records at the time of first echocardiographic investigation.

Cardiac adverse events such as sustained ventricular tachyarrhythmia, hospital admission due to heart failure (HF), need for surgery and death during the whole follow-up period were recorded.

Baseline clinical and instrumental features of EA patients with stable disease were compared with those of patients with progressive disease, experiencing cardiac adverse events.

The study was approved by the local Ethics Committee.

2.2. Standard echocardiographic analysis

The first transthoracic echocardiogram with good digitally stored images available between January 2005 and December 2017 for each patient was analyzed for offline assessment by an expert operator blinded to clinical and follow-up data, to extrapolate all standard and speckle tracking echo cardiac parameters. Three cardiac cycles stored in cine-loop format were used for off-line analysis and the measurements were averaged.

Right heart chambers were defined as following (all in apical 4-chamber view) [15,17]:

- Anatomical RV: the portion of functional RV + the atrialized portion of RV (between septal displaced TV leaflet and TV annulus) (Fig. 1A);
- Functional right ventricle (RV): the portion of RV distal to the attachment points of the TV leaflets (Fig. 1C);
- Native right atrium (RA): portion of RA above anatomical TV annulus (Fig. 1E).

Mitral annular plane systolic excursion (MAPSE) and tricuspid annular plane systolic excursion (TAPSE) were measured as described previously [18]. In order to account for differences in body size in pediatric patients, both MAPSE and TAPSE were indexed to LV and RV length, respectively [19].

Left ventricular ejection fraction (LVEF) was calculated using biplane Simpson's rule from the apical 4- and 2-chamber views; when 2-chamber view was not available, LVEF from 4-chamber view only was calculated. Fractional area change (FAC) was measured tracing RV area in diastole and systole in 4-chamber view for both anatomic and functional RV, defined as previously described [20].

Native RA and left atrium (LA) volumes indexed for BSA were measured [20].

Mitral inflow *E*- and A-wave peak velocities, E-wave deceleration time, early (e′) diastolic tissue-Doppler myocardial velocities at the septal and lateral corners of the mitral annulus were calculated [21].

Peak systolic tissue-Doppler myocardial velocity (s′) at the basal segment of the RV free wall in correspondence of TV annulus was calculated [22].

Grading of tricuspid regurgitation (TR) (grade 1 = trivial to mild, 2 = mild to moderate, 3 = moderate, 4 = severe) was based on the width of colour regurgitation jet at the valve level (vena contracta), the extent of the regurgitation jet in the RA and its size and volume, as recommended by the American Society of Echocardiography and European Society of Cardiovascular Imaging [23].

The Celermajer index was calculated as the ratio of the combined area of the RA and the atrialized portion of RV to that of the functional RV and left heart in a four-chamber view at end-diastole. This ratio is used to define four grades of increasing severity of EA: ratio <0.5 = grade 1, ratio 0.5 to 0.99 = grade 2, ratio 1 to 1.49 = grade 3 and ratio ≥1.5 = grade 4 [24].

The Carpentier's classification was defined as following: type A, the volume of the true right ventricle is adequate; type B, a large atrialized component of the right ventricle exists, but the anterior leaflet of the TV moves freely; type C, the anterior leaflet is severely restricted in its movement and may cause significant obstruction of the right ventricular outflow tract; and type D, almost complete atrialization of the ventricle except for a small infundibular component [25].

2.3. 2D-Speckle tracking echocardiographic analysis

Speckle tracking echocardiographic (STE) analysis was performed using a commercially available vendor independent software package (2D Cardiac Performance Analysis Software, TomTec, Unterschleissheim, Germany).

The best apical four-chamber view to visualize the segments of each ventricle was selected. Briefly, 3 points (2 annular and 1 apical) were positioned enabling the software to track the myocardium semi-automatically throughout the heart cycle. The region of interest was adjusted with careful inspection of tracking and manual correction, if needed, was performed. The automated algorithm allowed global longitudinal strain (GLS) to be calculated.

Left ventricle longitudinal (LV-GLS) and right ventricle longitudinal (RV-GLS) strain by speckle tracking were defined as the average peak negative value on the strain curve during the systole (end of T-wave on the ECG) [26]. Particularly, for RV-GLS, both anatomic (Fig. 1B) and functional (Fig. 1D) RV strain were acquired.

Native RA strain by speckle tracking was also detected [27]. RA strain was assessed in the same echocardiographic projections used for RV-GLS quantification; endocardial border was traced manually and adjusted to the RA wall, resulting in strain curves from a total of 3 atrial segments and the average was used for the analysis. Global peak atrial longitudinal strain (PALS) of native RA was defined as the maximum positive strain value during LV systole (Fig. 1F). Frame rates for speckle tracking loops ranged from 60 to 85 fps.

2.4. Follow-up

Cardiac adverse events such as death, sustained ventricular tachyarrhythmia, heart failure, and need for surgery during the follow-up period were recorded:

- Sustained ventricular tachyarrhythmia was defined as ventricular tachycardia lasting at least 30 s, ventricular tachycardia associated with pre-syncope/syncope or ventricular fibrillation;
- Heart failure was defined as admission for diuresis of fluid overload not secondary to acute arrhythmia presentation [17];
- Need for surgery (Cone procedure and/or surgical tricuspid valve replacement and/or other surgical procedures) was based on symptoms worsening or the presence of severe tricuspid regurgitation and severe right heart dilatation [28].

Follow-up time was calculated from the time of the first transthoracic echocardiography with adequate digitally stored images until last clinical visit or death.

2.5. Statistical analysis

The normal distribution of continuous variables was verified using the Kolmogorov-Smirnov goodness-of-fit test. Continuous variables with normal distribution were presented as mean ± standard deviation (SD) and those with non-normal distribution were presented as median (interquartile range, 25th and 75th percentile). Categorical variables were presented as frequency (percentage).

Continuous variables were then compared by using the unpaired Student's *t*-test or the Mann-Whitney *U* test, as appropriate. Categorical variables were compared with chi-square statistics or a Fisher exact test, as appropriate.

Ascending stepwise logistic regression was used to determine the echocardiographic independent risk factors of progressive disease during the whole follow-up period. We used a parsimonious model including variables with $p < 0.01$ by univariate test as candidates for the multivariate analysis [29].

Receiver-operating characteristic (ROC) curve analyses were performed to determine the areas under the curves for independent risk factors detected by ascending stepwise logistic regression, and optimal cutoffs were selected by optimizing sensitivity plus specificity.

Cumulative survival curves were performed using the Kaplan-Meier method and the difference between groups was assessed by log-rank test. Statistical significance was established at $p < 0.05$. Statistical analysis was performed using SPSS version 23.0 statistical software (SPSS Inc., Chicago, Illinois).

2.6. Reproducibility study

Inter-observer variability for myocardial deformation properties was assessed in 10 randomly selected studies and was calculated as the ratio (expressed as a percentage) of the difference between the values obtained by each observer (expressed as an absolute value) divided by the mean of the two values and as intra-class correlation coefficients. Intra-observer variability was calculated by a similar approach.

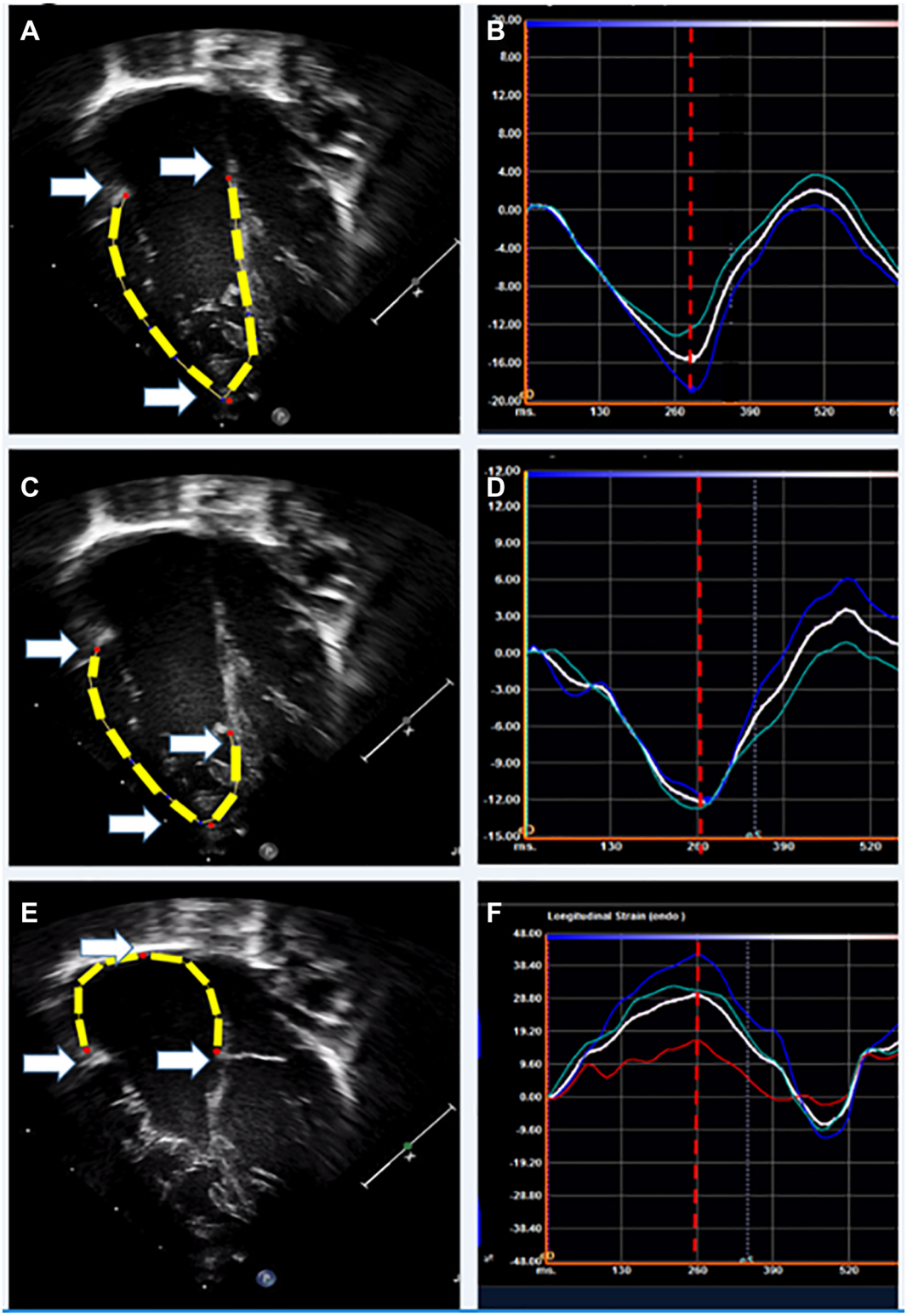

Fig. 1. Representative right heart chambers evaluation and speckle tracking-derived strain curves in Ebstein's anomaly patients. A) Anatomic right ventricle (RV): the portion of functional RV + the atrialized portion of RV (between displaced tricuspid valve septal leaflet and annulus); C) Functional RV: the portion of RV distal to the attachment points of the tricuspid valve leaflets; (E) Native right atrium (RA): portion of RA above tricuspid valve annulus. RV global longitudinal strain (GLS) defined as the average peak negative value on the strain curve during left ventricular (LV) systole (red dotted lines) was detected for both anatomic (B) and functional (D) RV. Atrial peak longitudinal strain (PALS), as the maximum positive strain value on the strain curve during LV systole (red dotted line) was detected for native RA (F). White arrows show marker points positioned by operators to enable the software to track the myocardium semi-automatically throughout the heart cycle in strain detection for both RV ventricle (A and C) and RA (E).

3. Results

3.1. Patients characteristics

A total of 58 consecutive pediatric and young adult EA patients met the inclusion criteria. In 8 patients, the image quality was not considered adequate for speckle tracking analysis and they were excluded from the study. Thus, 50 patients (age range 1 day–18 years, median 4; 52% males) were included in the study and were followed for a mean follow-up of 60 ± 41 months (range 1–147 months).

During the whole period, 24 (48%) EA patients had progressive disease, experiencing cardiac adverse events at a median age of 69 months (IQR 2–196.25 months). Particularly, 18 patients (36% of overall population) underwent surgical intervention, 1 (2%) experienced sustained VT and 5 (10%) needed hospital admission for HF; two of these HF patients died.

Among patients who underwent surgical intervention, 14 (77.8%) underwent a Cone repair; three (16.7%) patients had a TV replacement; one (5.5%) patient underwent a TV repair with a one and a half ventricle strategy and completed a total cavo-pulmonary connection seven years later.

At baseline investigation, all EA patients were in NYHA Class I and had sinus rhythm at ECG; 18 (36%) had a documented past medical history of supraventricular tachyarrhythmia, among those 11 (22% of overall population) presented with pre-excitation syndrome. Baseline patients' characteristics are summarized in Table 1.

Patients with stable and progressive disease were comparable for all the studied parameters except for resting oxygen saturation, which was lower in patients experiencing adverse events (oxygen saturation ≤90%: 45% vs 0% in stable vs progressive disease group; $p < 0.001$).

3.2. Standard echocardiographic study

3.2.1. Right chambers

Table 2 summarizes the standard and advanced studied echocardiographic parameters.

Anatomic severity of EA patients was variable in the overall studied population; grade of displacement of TV septal leaflet ranged from 8.8 to 13.3 mm/m^2, with a median of 39.2 mm/m^2 (IQR 25.8–69.7). A more severe grade of displacement was detected in progressive disease group compared to stable patient [59.7 mm/m^2 (IQR 27.5–83) vs 28.4 mm/m^2 (IQR 17.5–47); $p = 0.002$].

No differences were detected in anatomic RV-FAC, in TAPSE/RV length and in peak systolic tissue-Doppler myocardial velocity (s') between EA patients with stable disease vs. those with progressive disease. Patients with progressive disease exhibited a lower functional RV-FAC mean value (29.2 ± 7.7% vs 36.7 ± 9.6%; $p = 0.004$).

Native RA volumes were increased in both stable and progressive disease groups [23.8 ml/m2 (IQR 16.3–36.8) vs 35.5 ml/m2 (IQR 19.6–60.1); $p = 0.065$].

About tricuspid valve regurgitation (TR), no significant differences in valve disease severity were detected between the two groups except for grade 2 TR, more frequent in stable disease group compared to the progressive one (53.8% vs 25%; $p = 0.048$). Only 4 patients showed a severe grade 4 TR and 3 were in the progressive disease group (12.5% vs 3.8%; $p = 0.340$).

Patients experiencing adverse cardiac events showed a higher Celermajer index [0.8 (IQR 0.7–0.98) vs 0.55 (IQR 0.4–0.7); $p = 0.000$].

No significant differences were detected in Carpentier's classification between the two groups.

Three patients (6% of overall population) showed functional pulmonary atresia and they all belonged to stable disease group (11.5% vs 0%; $p = 0.236$).

3.2.2. Left chambers

Systolic function of the left ventricle was preserved in the overall population, showing similar values of LVEF between patients with progressive and stable disease (55.6 ± 9.4% vs 59.7 ± 7.5%; $p = 0.09$). MAPSE corrected for LV length was similar between the two groups.

No differences were found between groups in the studied LV diastolic parameters as well as in LA volumes indexed for body surface area.

3.3. 2D-speckle tracking echocardiographic study

Functional RV-GLS and anatomic RV-GLS were respectively −13.3 ± 7.3% and − 14.4 ± 5.9% in the overall population. Functional RV-GLS showed a significantly reduced value in EA patients with progressive disease compared with the stable ones (−10.2 ± 6.2% vs −16.2 ± 7.3%; $p = 0.003$).

Native RA-PALS in EA patients experiencing adverse cardiac events was significantly lower than in patients with stable disease (25.2 ± 13.5% vs 36.3 ± 12.5%; $p = 0.004$).

Despite preserved LVEF, mean value of LV-GLS of overall population was slightly reduced (−16.1 ± 4.2%). Patients with progressive disease showed lower LV-GLS than patients with stable disease (−14.5 ± 3.9% vs −17.5 ± 4%; $p = 0.011$).

3.4. Prognostic values of echo parameters

On multivariate analysis, including parameters significantly different ($p < 0.01$) at univariate analysis (Celermajer index, TV displacement/BSA, functional RV FAC, functional RV GLS and native

Table 1
Demographic and clinical characteristics of study population.

	All patients (N = 50)	Patients with stable disease ($n = 26$)	Patients with progressive disease ($n = 24$)	p-Value
Age, years[a]	4 (0.01–15)	7.5 (1.5–15.25)	1.35 (0.005–13.5)	0.069
Males, n (%)	26 (52)	11 (42.3)	15 (62.5)	0.153
BSA, mm/m^2[a]	0.67 (0.21–1.7)	0.82 (0.45–1.72)	0.5 (0.21–1.63)	0.115
Sinus rhythm, n (%)	50 (100)	26 (100)	24 (100)	/
NYHA class I, n (%)	50 (100)	26 (100)	24 (100)	/
SBP, mmHg	107.6 ± 9.2	105.8 ± 11	109.4 ± 7.8	0.567
DBP, mmHg	61.6 ± 8.2	62.2 ± 9.8	61 ± 7.2	0.832
SatO2 < 90%, n(%)	9 (21.4)	0	9 (45)	**0.000**
QRS duration >110 msec, n (%)	21 (45)	13 (52)	8 (40)	0.423
Cardio-thoracic ratio > 0.6, n (%)	22 (52.4)	8 (40)	14 (63.6)	0.126
Previously documented tachyarrhythmia, n(%)	18 (36)	9 (34.6)	9 (37.5)	0.832
Pre-excitation syndrome at EP study, n (%)	11 (22)	8 (30.8)	3 (12.5)	0.119

BSA: body surface area; NYHA: New York Heart Association; SBP = systolic blood pressure; DBP = diastolic blood pressure; SatO2 = oxygen saturation; EP study: electrophysiological study.

[a] Expressed as median (IQR).

Table 2
Standard and advanced echocardiographic features of study population.

	All patients ($N = 50$)	Patients with stable disease ($N = 26$)	Patients with progressive disease ($N = 24$)	p-Value
Right heart chambers				
Displacement of TV/BSA, mm/m^2[a]	39.2 (25.8–69.7)	28.4 (17.5–47)	59.7 (27.5–83)	**0.002**
TAPSE/RV length, %	0.3 ± 0.1	0.3 ± 0.08	0.3 ± 0.11	0.142
FAC functional RV, %	33.1 ± 9.5	36.7 ± 9.6	29.2 ± 7.7	**0.004**
FAC anatomic RV, %	35.2 ± 8.7	33.1 ± 9.2	37.5 ± 7.7	0.073
TDI s' RV, cm/s	12.8 ± 4.6	13.3 ± 2.4	11.7 ± 8.1	0.639
Native RA vol/BSA, ml/m^2[a]	28.2 (18.3–46.5)	23.8 (16.3–36.8)	35.5 (19.6–60.1)	0.065
TR V max, m/s	2.4 ± 0.4	2.5 ± 0.4	2.4 ± 0.5	0.303
Grading TR:				
1, n(%)	1 (2)	1 (3.8)	0 (0)	1
2, n(%)	20 (40)	14 (53.8)	6 (25)	**0.048**
3, n(%)	25 (50)	10 (38.5)	15 (62.5)	0.156
4, n(%)	4 (8)	1 (3.8)	3 (12.5)	0.340
Left heart chambers				
LVEF, %	57.7 ± 8.6	59.7 ± 7.5	55.6 ± 9.4	0.089
MAPSE-s/LV length, %	0.19 ± 0.05	0.18 ± 0.05	0.19 ± 0.06	0.532
MAPSE-l/LV length, %	0.21 ± 0.06	0.21 ± 0.05	0.22 ± 0.07	0.591
LA vol/BSA, ml/m^2	17.1 ± 7.3	16.6 ± 5.9	17.7 ± 8.6	0.602
E/A ratio	1.25 ± 0.5	1.4 ± 0.6	1.1 ± 0.4	0.064
E/è ratio	7.9 ± 3.8	7.4 ± 2.9	8.9 ± 5.2	0.514
Celermajer index[a]	0.68 (0.53–0.87)	0.55 (0.38–0.69)	0.8 (0.70–0.98)	**0.000**
Carpentier's classification				
A, n(%)	9 (18)	7 (26.9)	2 (8.3)	0,142
B, n(%)	25 (50)	15 (57.7)	10 (41.7)	0,258
C, n(%)	6 (12)	1 (3.8)	5 (20.8)	0,093
D, n(%)	10 (20)	3 (11.5)	7 (29.2)	0,164
Advanced echo				
Anatomic RV GLS, %	−14.4 ± 5.9	−15.5 ± 6.3	−13.2 ± 5.3	0.165
Functional RV GLS, %	−13.3 ± 7.3	−16.2 ± 7.2	−10.2 ± 6.2	**0.003**
RA-PALS, %	30.9 ± 14	36.3 ± 12.5	25.2 ± 13.5	**0.004**
LV-GLS, %	−16.1 ± 4.2	−17.5 ± 4	−14.5 ± 3.9	**0.011**

TV: tricuspid valve; BSA: body surface area; TAPSE: tricuspid annular plane systolic excursion; RV: right ventricle; FAC: fractional area change; TDI s': peak systolic tissue-Doppler myocardial velocity; RA: right atrium; TR: tricuspid regurgitation; LVEF: left ventricular ejection fraction; MAPSE-s: septal mitral annular plane systolic excursion; MAPSE-l: lateral mitral annular plane systolic excursion; LA: left atrium; GLS: global longitudinal strain; PALS: peak atrial longitudinal strain.
[a] Expressed as median (IQR).

RA-PALS), only functional RV-FAC (OR: 0.886, 95% CI: 0.808–0.971; $p = 0.010$) and RA-PALS (OR: 0.926, 95% CI: 0.874–0.980, $p = 0.009$) were independent predictors of progressive disease in EA patients.

The ROC analysis for both functional RV-FAC and RA-PALS were shown in Fig. 2A.

The optimum cut-off points were: 31.5% for the RV-FAC, with a sensitivity of 67% and a specificity of 77% and an area under the curve of 0.730; 27.1% for native RA-PALS, with a sensitivity of 63% and a specificity of 81% and an area under the curve of 0.749.

Cumulative survival curves were constructed using the Kaplan-Meier method (Fig. 2B). Patients with both functional RV-FAC ≥ 31.5%

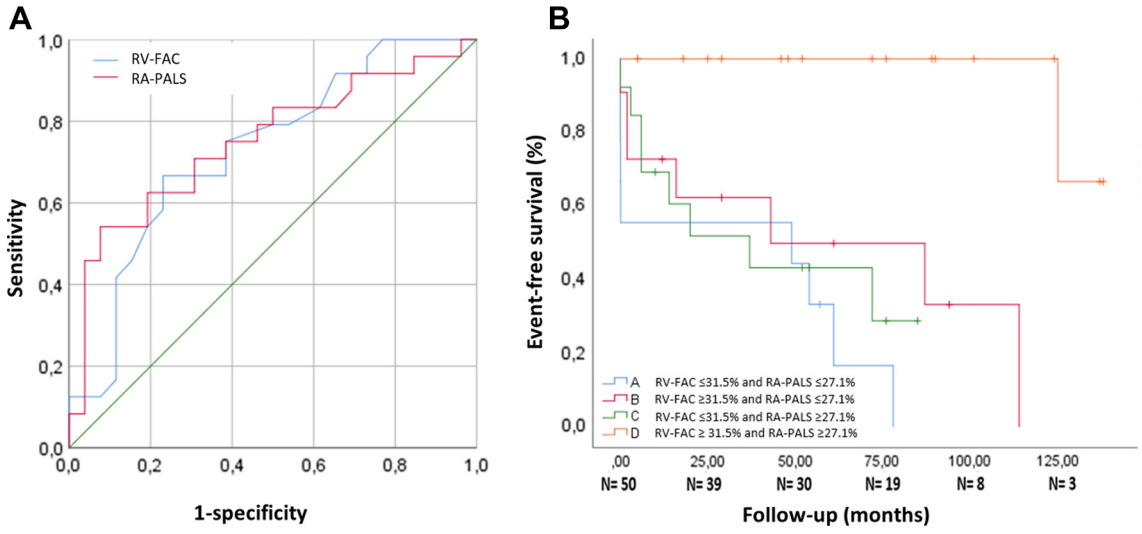

Fig. 2. ROC curves for functional RV fractional area change (FAC) and native RA-PALS (A). Cumulative survival curves were constructed using the Kaplan-Meier method: patients were stratified according to functional RV FAC and native RA strain cut-off points which emerged from ROC analysis (B).

and native RA-PALS ≥27.1% showed significantly increased event-free survival compared to patients with both values under the cut-off points ($p = 0.000$).

3.5. Reproducibility analysis

Intra- and inter-observer variability expressed as the mean percentage error (absolute difference/mean) and the intra-class correlation coefficients (ICC) were good for all studied parameters: TAPSE/RV length (20 ± 17% and 21 ± 15%, respectively; ICC: 0.89 and 0.87 respectively); functional RV-FAC (11 ± 7% and 13 ± 8%; ICC: 0.89 and 0.87); anatomic RV-GLS (25 ± 23% and 25 ± 22%; ICC: 0.84 and 0.83); functional RV-GLS (22 ± 15% and 23 ± 16%; ICC: 0.89 and 0.88); native RA-PALS (13 ± 12% and 14 ± 12%; ICC: 0.93 and 0.91); LV-GLS (19 ± 15% and 19 ± 16%; ICC: 0.83 and 0.82).

4. Discussion

To the best of our knowledge, this is the first study to investigate the prognostic value of both atrial and ventricular myocardial deformation properties in pediatric and young patients with unrepaired Ebstein's anomaly.

Our findings show that the function of both right atrium and right ventricle are independent predictors of progressive disease in EA patients.

4.1. Predictors of outcome in Ebstein's anomaly patients

Previous studies focused on the predictive value of several clinical and instrumental parameters on adverse outcome in EA patients with rather conflicting results [6–10]. Recently, CMR-derived changes in biventricular function parameters have been reported to be associated with adverse cardiac events in adult EA patients [17]. Another recent CMR study showed that EA patients had significantly impaired right atrial and ventricular performance, which correlated well with heart failure parameters [30].

Unfortunately, the use of CMR is limited in the pediatric population. In children (≤10 years) a CMR examination often requires general anesthesia; the high cost and limited availability are additional limitations for this technique [31].

Data focused on echocardiography and its prognostic value in unrepaired EA patients are still scarce in the literature, even more so in a pediatric population [13,14].

Our study is the first to investigate the role of standard and advanced echocardiographic parameters in predicting outcome in pediatric and young EA patients.

4.2. Right ventricle in EA disease

In EA the anatomic RV includes an atrialized part that functionally belong to the atrium and doesn't contribute properly to global systolic function of right heart [32].

In agreement with this, our findings demonstrated that only the echocardiographic assessment of functional RV-FAC has a prognostic value in EA patients.

Attenhofer et al. [33] could not measure FAC in any of the 16 adult studied patients (mean age 41 ± 13 years; 3 patients with previous surgery) because of difficulties in detecting the RV endocardial borders. On the contrary, in our study it was feasible in all patients, probably due to the inclusion only of unrepaired children and young adults (≤18 years), who usually have a good image quality.

A higher Celermajer index and a more severe TV displacement/BSA were also detected in patients with progressive disease. However, at multivariate analysis no statistical significance was reached. This could confirm the greater importance of function rather than morphology of RV in prognostic assessment of EA patients.

In a recent study about changes in biventricular function after Cone repair in children and adult patients, Perdreau et al. concluded that STE of RV was not feasible due to dilatation and little thickness of myocardial RV wall [28]. However, longitudinal strain reflects the shortening of myocardial fibers along the longitudinal axis. To measure the longitudinal deformation, the STE software follows the myocardial speckles along the longitudinal axes, and not along the transverse axes. Thus, the myocardial wall thickness on the transverse plane should not affect the quality of the tracking [26]. Indeed, many studies demonstrated the feasibility of speckle tracking in assessing the longitudinal deformation of the extremely thin atrial walls in several heart diseases [27,34]. In our patients, RV-GLS was feasible for the optimal image quality of unrepaired young patients, showing lower mean value in EA patients with progressive disease compared to the stable ones. In agreement with our findings, another recent study in EA children and adult patients demonstrated that only RV GLS, assessed by echo, was well correlated to RV ejection fraction detected by CMR [15].

At multivariate analysis functional RV-GLS lost statistical significance, probably because FAC is a more powerful parameter. The contraction of both obliquely and longitudinally oriented RV myocardial fibers is responsible for RV systolic function. In cases of abnormal loading conditions, like in EA, circumferential shortening may contribute more to RV ejection than in normal hearts [35]. We hypothesized that RV-GLS, expression of shortening of longitudinally oriented myocardial fibers, is already compromised in all EA young patients, while FAC may be maintained because of a compensatory increase in circumferential deformation, expression of the contraction of the obliquely oriented fibers. Thus, a reduced FAC may be the expression of a later stage in the disease progression, when both longitudinal and circumferential function are compromised.

In our study we did not assess RV circumferential deformation because the thin wall may significantly affect the quality of tracking on the transverse axis.

4.3. Right atrium in EA disease

Quantification of RA function in congenital heart disease is receiving increasing interest, since RA dysfunction may better reflect diastolic properties of RV [34,36,37]. As RV dysfunction progresses because of RV volume overload, the preload reserve responds through compensation by the atrium; when RA compensation is exhausted, than the cardiac output decreases [38]. Padeletti et al. reported that RA-PALS was the strongest predictor of pulmonary hypertension in patients with heart failure [39]. Similarly, we evaluated RA function in EA patients by focusing on the reservoir phase, demonstrating for the first time that RA function detected by STE is an independent predictor of progressive disease at long-term follow-up.

4.4. Left ventricle in EA

It is well known that RV volume overload leads to a reduction of global systolic LV function through the mechanism of ventricular interdependence [40]. Moreover, LV dysfunction in EA is an independent predictor of late mortality [41].

Our findings showed that, despite normal LVEF, patients with progressive disease showed a lower LV-GLS average value compared to patients with stable disease.

These results are in agreement with a recent paper by Liu et al. [42] showing CMR-detected LV strain parameters were significantly lower in EA patients compared to control group even in presence of a normal LVEF. The abnormal LV longitudinal deformation is probably due to an early involvement of the sub-endocardial longitudinally oriented fibers, which are the first to be compromised even in presence of a preserved LVEF [43,44].

5. Study limitations

There are several limitations concerning this study.

The first limitation is related to the retrospective design of the study.

Secondly, the sample size may seem small. However, considering the incidence of EA, the single-center nature of the study, the inclusion criteria, and the involvement of only pediatric and young adult patients (≤18 years), the studied cohort can be considered relatively large. Indeed, our EA sample size is the largest as compared with all previous studies on this specific topic [13–15,33].

Third, we used two-dimensional strain to assess myocardial deformation properties in EA patients. However, strain is not a direct measure of contractility, whereas strain rate is more closely related to myocardial contractility. Unfortunately, strain rate cannot be fully resolved from STE because of its relatively low frame rate. A reliable measure of myocardial strain rate can be assessed only by colour tissue Doppler (frame rate > 180 frames/s), but this approach is limited by poor reproducibility [45].

In addition, in our study the specificity and sensitivity of RV-FAC and RA-PALS are not very high thus their predictive value should be confirmed in a larger multicenter study. Similarly, both "functional" pulmonary atresia and the severity of TR don't reach a significant value in predicting cardiovascular events but these results can be partially explained by the relative small number of patients affected.

6. Conclusion

Our study demonstrates for the first time the prognostic role of functional RV-FAC and native RA-PALS in long-term follow-up of pediatric and young adult EA patients. We therefore suggest that these two parameters should be included in the routine clinical evaluation of children and young patients with EA.

Conflict(s) of interest/disclosures

No conflict of interest to declare.

References

[1] C.H. Attenhofer Jost, H.M. Connolly, J.A. Dearani, W.D. Edwards, G.K. Danielson, Ebstein's anomaly, Circulation 115 (2007) 277–285.
[2] S. Fratz, C. Janello, D. Müller, et al., The functional right ventricle and tricuspid regurgitation in Ebstein's anomaly, Int. J. Cardiol. 167 (2013) 258–261.
[3] H. Watson, Natural history of Ebstein's anomaly of tricuspid valve in childhood and adolescence: an international co-operative study of 505 cases, Br. Heart J. 36 (1974) 417–427.
[4] D.S. Celermajer, C. Bull, J.A. Till, et al., Ebstein's anomaly: presentation and outcome from fetus to adult, J. Am. Coll. Cardiol. 23 (1994) 170–176.
[5] J.A. Dearani, B.N. Mora, T.J. Nelson, D.T. Haile, P.W. O'Leary, Ebstein anomaly review: what's now, what's next? Expert. Rev. Cardiovasc. Ther. 13 (2015) 1101–1109.
[6] J. Radojevic, R. Inuzuka, R. Alonso-Gonzalez, et al., Peak oxygen uptake correlates with disease severity and predicts outcome in adult patients with Ebstein's anomaly of the tricuspid valve, Int. J. Cardiol. 163 (2013) 305–308.
[7] E.N. Oechslin, D.A. Harrison, M.S. Connelly, G.D. Webb, S.C. Siu, Mode of death in adults with congenital heart disease, Am. J. Cardiol. 86 (2000) 1111–1116.
[8] M.L. Brown, J.A. Dearani, G.K. Danielson, et al., Functional status after operation for Ebstein anomaly: the Mayo Clinic experience, J. Am. Coll. Cardiol. 52 (2008) 460–466.
[9] F. Attie, M. Rosas, M. Rijlaarsdam, et al., The adult patient with Ebstein anomaly. Outcome in 72 unoperated patients, Medicine 79 (2000) 27–36.
[10] G. Egidy Assenza, A.M. Valente, T. Geva, et al., QRS duration and QRS fractionation on surface electrocardiogram are markers of right ventricular dysfunction and atrialization in patients with Ebstein anomaly, Eur. Heart J. 34 (2013) 191–200.
[11] O.J. Booker, N.C. Nanda, Echocardiographic assessment of Ebstein's anomaly, Echocardiography 32 (Suppl. 2) (2015) S177–S188.
[12] M.Y. Qureshi, P.W. O'Leary, H.M. Connolly, Cardiac imaging in Ebstein anomaly, Trends Cardiovasc Med. 28 (2018 Jan 12) 403–409.
[13] J. Therrien, M.Y. Henein, W. Li, J. Somerville, M. Rigby, Right ventricular long axis function in adults and children with Ebstein's malformation, Int. J. Cardiol. 73 (2000) 243–249.
[14] B.W. Eidem, C. Tei, P.W. O'Leary, F. Cetta, J.B. Seward, Nongeometric quantitative assessment of right and left ventricular function: myocardial performance index in normal children and patients with Ebstein anomaly, J. Am. Soc. Echocardiogr. 11 (1998) 849–856.
[15] A. Kühn, C. Meierhofer, T. Rutz, et al., Non-volumetric echocardiographic indices and qualitative assessment of right ventricular systolic function in Ebstein's anomaly: comparison with CMR-derived ejection fraction in 49 patients, Eur. Heart J. Cardiovasc. Imaging 17 (8) (2016) 930–935.
[16] W.D. Edwards, Embryology and pathologic features of Ebstein's anomaly, Prog. Pediatr. Cardiol. 2 (1993) 5–15.
[17] R. Rydman, Y. Shiina, G.P. Diller, et al., Major adverse events and atrial tachycardia in Ebstein's anomaly predicted by cardiovascular magnetic resonance, Heart 104 (2018) 37–44.
[18] M.Y. Henein, D.G. Gibson, Normal long axis function, Heart 81 (1999) 111–113.
[19] Z. Issa, N.J. Moiduddin, Z. Bulbul, G. Di Salvo, New echocardiogram index alternatives to MAPSE and TAPSE z-scores in children, J Saudi Heart Assoc 27 (2015) 299–333.
[20] R.M. Lang, L.P. Badano, V. Mor-Avi, Recommendations for cardiac chamber quantification by echocardiography in adults: an update from the American Society of Echocardiography and the European Association of Cardiovascular Imaging, J. Am. Soc. Echocardiogr. 28 (2015) 1–39.
[21] S.F. Nagueh, O.A. Smiseth, C.P. Appleton, et al., Recommendations for the evaluation of left ventricular diastolic function by echocardiography: an update from the American Society of Echocardiography and the European Association of Cardiovascular Imaging, Eur. Heart J. Cardiovasc. Imaging 17 (2016) 1321–1360.
[22] F. Weidemann, B. Eyskens, F. Jamal, et al., Quantification of regional left and right ventricular radial and longitudinal function in healthy children using ultrasound-based strain rate and strain imaging, J. Am. Soc. Echocardiogr. 15 (2002) 20–28.
[23] P. Lancellotti, C. Tribouilloy, A. Hagendorff, et al., Recommendations for the echocardiographic assessment of native valvular regurgitation: an executive summary from the European Association of Cardiovascular Imaging, Eur. Heart J. Cardiovasc. Imaging 14 (2013) 611–644.
[24] D.S. Celermajer, S. Cullen, I.D. Sullivan, et al., Outcome in neonates with Ebstein anomaly, J. Am. Coll. Cardiol. 19 (1992) 1041–1046.
[25] A. Carpentier, S. Chauvaud, L. Mace, et al., A new reconstructive operation for Ebstein's anomaly of the tricuspid valve, J. Thorac. Cardiovasc. Surg. 96 (1988) 92–101.
[26] J.U. Voigt, G. Pedrizzetti, P. Lysyansky, et al., Definitions for a common standard for 2D speckle tracking echocardiography: consensus document of the EACVI/ASE/industry task force to standardize deformation imaging, Eur. Heart J. Cardiovasc. Imaging 16 (2015) 1–11.
[27] R. Vianna-Pinton, C.A. Moreno, C.M. Baxter, K.S. Lee, T.S. Tsang, C.P. Appleton, Two-dimensional speckle-tracking echocardiography of the left atrium: feasibility and regional contraction and relaxation differences in normal subjects, J. Am. Soc. Echocardiogr. 22 (2009) 299–305.
[28] E. Perdreau, V. Tsang, M.L. Hughes, Change in biventricular function after cone reconstruction of Ebstein's anomaly: an echocardiographic study, Eur. Heart J. Cardiovasc. Imaging 0 (2017) 1–8.
[29] S.K. Sarkar, H. Midi, S. Rana, Model selection in logistic regression and performance of its predictive ability, Aust. J. Basic Appl. Sci. 4 (2010) 5813–5822.
[30] M. Steinmetz, M. Broder, O. Hösch, et al., Atrio-ventricular deformation and heart failure in Ebstein's anomaly - a cardiovascular magnetic resonance study, Int. J. Cardiol. 257 (2018 Apr 15) 54–61.
[31] Valsangiacomo Buechel ER, Grosse-Wortmann L, Fratz S et al. Indications for cardiovascular magnetic resonance in children with congenital and acquired heart disease: an expert consensus paper of the imaging working group of the AEPC and the cardiovascular magnetic resonance section of the EACVI. Eur. Heart J. Cardiovasc. Imaging, vol 16, no. 3, pp. 281–297.
[32] K.R. Anderson, J.T. Lie, The right ventricular myocardium in Ebstein's anomaly. A morphometric histopathologic study, Mayo Clin Proc 54 (1979) 181–184.
[33] C. Attenhofer Jost, D. Whitney, P.R. Julsrud, et al., Prospective comparison of echocardiography versus cardiac magnetic resonance imaging in patients with Ebstein's anomaly, Int. J. Card. Imaging 28 (2012) 1147–1159.
[34] G. Di Salvo, M. Drago, G. Pacileo, et al., Atrial function after surgical and percutaneous closure of atrial septal defect: a strain rate imaging study, J. Am. Soc. Echocardiogr. 18 (2005) 930–933.
[35] E.R. Valsangiacomo Buechel, L.L. Mertens, Imaging the right heart: the use of multimodality imaging, Eur. Heart J. 33 (2012) 940–960.
[36] E. Riesenkampff, N. Al-Wakeel, S. Kropf, et al., Surgery impacts right atrial function in tetralogy of Fallot, J. Thorac. Cardiovasc. Surg. 147 (2014) 1306–1311.
[37] S. Cakal, E. Eroglu, O. Baydar, et al., Two-dimensional strain and strain rate imaging of the left atrium and left ventricle in adult patients with atrial septal defects before and after the later stage of percutaneous device closure, Echocardiography 32 (2014) 470–474.
[38] K. Sakata, Y. Uesugi, A. Isaka, et al., Evaluation of right atrial function using right atrial speckle tracking analysis in patients with pulmonary artery hypertension, J. Echocardiogr. 14 (2016) 30–38.
[39] M. Padeletti, M. Cameli, M. Lisi, et al., Right atrial speckle tracking analysis as a novel noninvasive method for pulmonary hemodynamics assessment in patients with chronic systolic heart failure, Echocardiography 28 (2011) 658–664.
[40] J. Müller, A. Kühn, M. Vogt, C. Schreiber, J. Hess, A. Hager, Improvements in exercise performance after surgery for Ebstein anomaly, J. Thorac. Cardiovasc. Surg. 141 (2011) 1192–1195.
[41] M.L. Brown, J.A. Dearani, G.K. Danielson, et al., Effect of operation for Ebstein anomaly on left ventricular function, Am. J. Cardiol. 102 (2008) 1724–1727.

[42] X. Liu, Q. Zhang, Z.G. Yang, Assessment of left ventricular deformation in patients with Ebstein's anomaly by cardiac magnetic resonance tissue tracking, Eur. J. Radiol. 89 (2017 Apr) 20–26.
[43] G. Di Salvo, G. Pacileo, E.M. Del Giudice, et al., Abnormal myocardial deformation properties in obese, nonhypertensive children: an ambulatory blood pressure monitoring, standard echocardiographic and strain rate imaging study, Eur. Heart J. 27 (2006) 2689–2695.
[44] J. Gorcsan, H. Tanaka, Echocardiographic assessment of myocardial strain, J. Am. Coll. Cardiol. 58 (2011) 1401–1413.
[45] G.R. Sutherland, G. Di Salvo, P. Claus, J. D'Hooge, B. Bijnens, Strain and strain rate imaging: a new clinical approach to quantifying regional myocardial function, J. Am. Soc. Echocardiogr. 17 (2004) 788–802.